Materials Today: Proceedings xxx (xxxx) xxx

Contents lists available at ScienceDirect

Materials Today: Proceedings

journal homepage: www.elsevier.com/locate/matpr

Synthesis of gamma biguanides butyric acid analogues as HDAC inhibitors and studying their cytotoxic activity

Othman Makki Sagheer [a,b,*], Mohammed Hassan Mohammed [b], Zaid O. Ibraheem [c], Jaafar S. Wadi [d], Mustafa F. Tawfeeq [d]

[a] Department of Pharmaceutical Chemistry, College of Pharmacy, Anbar University, Ramadi, Anbar, Iraq
[b] Department of Pharmaceutical Chemistry, College of Pharmacy, Baghdad University, Baghdad, Iraq
[c] Department of Pharmacy, Al Nsoor University College, Al Mustansyria, Baghdad, Iraq
[d] Department of Pharmaceutical Chemistry, College of Pharmacy, Tikrit University, Tikrit, Iraq

ARTICLE INFO

Article history:
Available online xxxx

Keywords:
HDAC
HDAC Inhibitors
Breast cancer
Biguanides
Cytotoxicity

ABSTRACT

Histone deacetylase (HDAC) inhibitors have been suggested as a new class of anticancer agents with promising effect on breast cancer. HDAC plays an important role in progression of breast cancer as it is overexpressed in the cancer cells. The study aimed at finding the HDAC inhibitory effect of three newly designed and synthesized hybrid molecules; made up of SAHA conjugated with the biguanid moiety of metformin. The molecules were amino[(E)-{amino[(4-anilino-4oxobutyl)amino] methylidene}amino] methaniminium chloride, amino[(E)-(amino{[4-(4-fluoroanilino)-4-oxobutyl] amino} methylidene) amino]methaniminium chloride, amino[(E)-(amino{[4-(4-chloroanilino)-4-oxobutyl]amino}methyli dene) amino] methaniminium chloride, (**7**–**9** respectively). Briefly, the plausible inhibitory effect against HDAC enzymes (HDAC1, HDAC2 and HDAC3) of the above mentioned compounds was deducted in *silico* using a chemo-informative simulation software programs, viz; SeeSAR and Chimera programs. Then, the compounds were synthesized, purified and identified using conventional synthetic and characterization methods. After that, their cytotoxic activity was determined against breast cancer using MCF-7 cell line and the results were compared with that of each of SAHA and metformin. The results revealed an appreciable cancer growth inhibition of all the synthesized analogues (IC_{50} range 161–72.5 μM). This suggests that these compounds could be a promising novel class of HADC inhibitors against breast cancer.

Selection and peer-review under responsibility of the scientific committee of the Technology Innovation in Mechanical Engineering-2021.

1. Introduction

Breast cancer is the most prevalent cancer among women at the postmenopausal age and rarely incurs in men. It a multifactorial disease with a high rate of mortality and morbidity [1,2]. Histone deacetylases enzymes (HDACs) are enzymes involved in the de-acetylation of the acetylated histone protein within the structure of chromatin fiber [3]. During the cellular activation, a cascade of transcription factors are produced and act on DNA to trigger genes expression. Their binding needs loss of the chromatin fibers compactness that can be achieved via histones acetylation through histone acetyl transferase enzyme [4]. This acetylation is balanced by the Histone Deacetylase enzyme (HDAC) which maintains the compactness of the chromatin fibers [5]. A dynamic balance between histone acetylation and de-acetylation is required to keep the cell in order and to do an epigenetic control on the genes expression [3]. Any imbalance between the two processes resulting in disruption of the feedback control of the cellular growth and proliferation resulting in enhancement of different types of cancers [6]. Some types of cancers are promoted via overexpression of HDAC enzyme resulting in histone deacetylation as this may results in suppression of the transcription factors involved in suppression or regulation of the cellular growth and proliferation. Breast cancer is a type of cancers; promoted by the enzymatic deacetylation of histone [7,8]. Interestingly, breast cancer cells show measurable levels of HDACs 1, 2, and 3 while normal breast cells do not show any and this may contribute the role of these enzymes in cancer development and progression [9,10]. This urged the scientists to propose HDAC inhibitors as candidate new drugs

* Corresponding author at: Department of Pharmaceutical Chemistry, College of Pharmacy, Anbar University, Ramadi, Anbar, Iraq.

https://doi.org/10.1016/j.matpr.2021.04.539
2214-7853/
Selection and peer-review under responsibility of the scientific committee of the Technology Innovation in Mechanical Engineering-2021.

in breast cancer therapy [8]. The aberrant silencing of genes in cancer may be associated with loss of histone acetylation. HDAC-inhibitors re-establish normal histone acetylation patterns in the breast cancer resulting in an anti-tumorigenic and an anti-metastasis effects characterized by the induction of the cell cycle arrest, apoptosis as well as cancer cells invasiveness and migration. These anti-proliferative effects are mediated by reactivation of silenced tumor suppressor genes [11–13]. Previous studies revealed a promising effect for the HDAC inhibitors against breast cancer [14,15]. Most of the zinc-dependent HDAC inhibitors like SAHA have common pharmacophores consisting of three distinct domains: (1) a surface recognition unit or cap group which usually a hydrophobic and aromatic group or may be heteroaromatic, which interacts with the rim of the binding pocket. (2) A zinc binding group (ZBG) or zinc binding domain (ZBD), such as the hydroxamic acid, benzamide or carboxylic acid groups, which coordinate with of Zn^{2+} ion in the active site. (3) A linker domain which is either saturated or unsaturated with linear or cyclic structure, that connects the cap group to the ZBD [16]. Besides the antidiabetic effect, metformin showed prominent anticancer properties with plausible mechanisms where its anticancer effect is suggested to be via its direct impact against some cellular targets [17], such as AMPK (Adenosine Monophosphate kinase) and mitochondria complex-I [18]. Furthermore, it can indirectly affects progression of cancer through its impact against development of the insulin resistance [19]. However, further studies are recommended to discover the exact mechanism of its action as anticancer agent [15,20].

The main objective of this study was primarily to design and synthesis novel class of HDAC inhibitors containing biguanides moieties through the generation of hybrid molecule [21] from fusion of two pharamcophoric structures, vorinostat and biguanide.

2. Materials and methods

2.1. Materials

The chemicals used in this study were boc-gamma aminobutyric acid (boc-GABA), aniline, 4-fluoroaniline, 4-chloroaniline, ethylchloroformate, triethylamine, dicyandiamide, trifluoroaceticacid, HCl

2.2. Drug design

The study aimed at discovering a new HDAC-I derived from hybridization of SAHA with a biguanide moiety and biological study to assess the activity of the newly synthesized analogues using in vitro cancer cell culture on MCF7 cell line of Her2 + breast cancer.

Accordingly a docking study was proposed to explore the most optimum pharmacophore among many designed molecules depending on HDAC-I SAR which are suspected to have appreciable activity on specific types of cancers like breast cancer by their HDAC inhibiting properties. According to the Structure activity relationship, the strategy was to design new class of non hydroxamic acid HDAC Inhibitors to achieve a good anticancer activity with the following potentials (a) the ability of biguanide to form many hydrogen bonds with the adjacent H-bond forming groups of amino acids like Histidine in the active site of HDAC enzyme, (b) anionic aspartate that could form strong ionic interaction with cationic biguanide moiety which is ionized in the physiological pH at the active site, (c) the interaction of biguanide group with zinc by forming coordinate bond is an appreciable goal [22,23].

2.3. In silico molecular docking study

Docking study selection is to be carried out using combination of SeeSAR, Chimera and ChimeraX tools to get appreciable realistic data about the designed analogues and which will be promising candidate to be synthesized experimentally.

2.4. Hybrid molecules synthesis is to be carried out by three steps

Amide coupling method which involves reaction of aniline, 4-fluoroaniline or 4-chloroaniline with free carboxylic group of N-protected amino acid (boc-GABA) forming N-protected amide using specific coupling reagent (Fig. 2). De-protection of the boc-amine to remove boc protecting group getting free amine using an acid catalyzed de-protection method. Coupling of free amine of the synthesized intermediate with dicyandiamide through acid catalyzed reaction resulting 3 of the designed analogues as mentioned above.

2.5. Synthesis of tert-butyl (4-anilino-4-oxobutyl) carbamate compound (1), (2) and (3)

Boc-GABA 10mmole (2.03 g) was dissolved in 50 ml DCM then 12mmole TEA was added then the solution cooled in ice bath to −5℃ in hood then ethylchloroformate (ECF) 12mmole added slowly with continuous stirring for thirty minutes then 10mmole of (aniline for **(1)** ,fluoroaniline for **(2)** and chloroaniline for **(3))** was dissolved in 10 ml DCM and then added dropwise to the mixture which left on stirring for 20 h, and then refluxed for three hours, the product then poured into separatory funnel and washed with 5% sodium bicarbonate solution, 5% HCl solution, Brine solution and finally with Distilled water many times, the organic layer was evaporated and the crude precipitated product was then triturated and washed with petroleum ether 40–60%, finally with ether to get white crystals [24].

2.6. Synthesis of 4-amino-N-phenylbutanamide HCl salt compound (4), (5) and (6)

From **(1), (2) or (3)** (5 mmol) was dissolved in 2 ml DCM containing anisole 10 mmole (1.1 ml) then 8 ml TFA was added slowly with continuous stirring at zero°C for forty minutes the success of deprotection was confirmed by TLC, then the mixture solvents were evaporated, the resulted crude product was washed with of acidic acetonitrile solution (acetonitrile 24.4 ml : 0.6 ml conc. HCl) and stirred, with time white crystals were appeared of HCl salt then filtration was done then washed with DCM and diethyl ether resulting white needle shaped crystals [25].

2.7. Synthesis of compounds (7), (8) and (9)

This step required dissolution of 3 mmole **(4), (5) or (6)** in 10 ml n-butanol then dicyandiamide 3.6 mmole (0.302 g) was added the mixture was refluxed for 20 h the reaction mixture was then poured into a beaker and dried then dissolved in 3 ml methanol then introduced into reversed phase preparative HPLC system [26–28] (Fig. 1).

2.8. Synthesized molecules purification, separation and characterization

Purification of the final products was done by using gradient reversed phase HPLC. The HPLC separation was achieved on C18 (250X10) and 5 μm particles size using gradient two solvents system, gradient mobile A (0.05% TFA in HPLC grade water) and mobile B (acetonitrile HPLC grade), firstly the optimization was

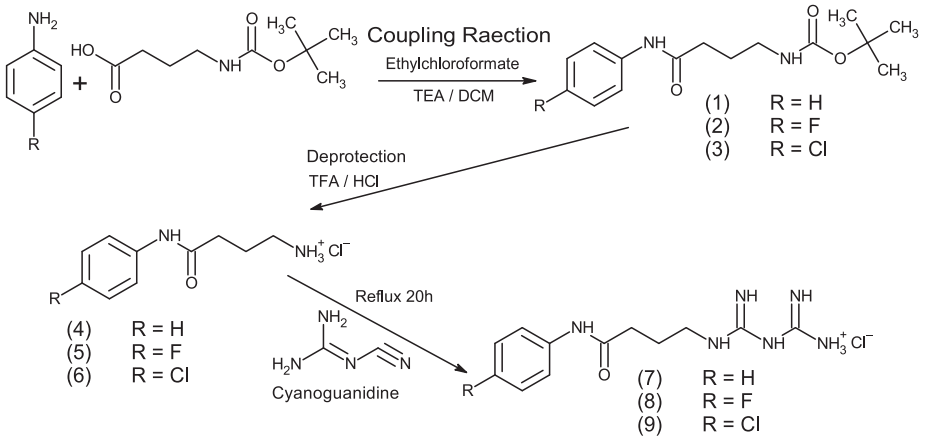

Fig. 1. Synthetic pathway.

done for each sample to get suitable gradient concentration and time resulting in an optimum separation pattern. The molecular characterization was done through TLC, Melting points, IR spectroscopy and HNMR studies [29,30].

2.9. Impact of the newly synthesized molecules on growth of MCF-7 cell line

MCF-7 cells were maintained in RPMI-1640 supplemented with 10% Fetal bovine serum, 100 units/mL penicillin, and 100 μg/mL streptomycin. Cells were passaged using Trypsin-EDTA reseeded at 80% confluence twice a week, and incubated at 37°C [31,32]. To determine the cytotoxic effect of compounds (**7**–**9**, SAHA and Metformin), the MTT tetrazolium assay was done using 96-well plates [33,34]. Cell lines were seeded at 1×10^4cells/well. After 24 h a confluent monolayer was achieved, cells were treated with analogues at five different concentration. Cell viability was measured after 72 h of treatment by removing the medium, adding 28 μL of 2 mg/mL solution of MTT and incubating the cells for 2.5 h at 37 °C. After removing the MTT solution, the crystals remaining in the wells were solubilized by the addition of 130 μL of DMSO followed by 37 °C incubation for 15 min with shaking [35]. The absorbency was determined on a microplate reader at 492 nm; the assay was performed in triplicate [36,37]. The inhibition rate of cell growth (the percentage of cytotoxicity) was calculated as the following equation percentage of growth inhibition = [(A-B)/A] * 100, wherein A is the optical density of control, and B is the optical density of the samples [38]. To visualize the shape of the cells under an inverted microscope, the cell were seeded into 24-well micro-titration plates at a density of 1×10^5 cells ml^{-1} and incubated for 24 h at 37 °C. Then, cells were exposed to test samples (7, 8, 9, SAHA and metformin) at IC50 concentration for 24hr. After the exposure time, the plates were stained with crystal violet stain and incubated at 37 °C for 10–15 min [36]. The stain was washed off gently with tap water until the dye was removed. The cells were observed under an inverted microscope [38–40].

3. Result and discussion

3.1. Characterization of the prepared materials

Based on the calculation of SeeSAR tool which provide a realistic ligand–protein interaction as estimated affinity values, these values have relied on HYDE[41] scoring method (estimates the free energy of binding based on dehydration and hydrogen bond). Upon docking of HDAC1 and by adjusting SeeSAR tool to obtain the maximum number of poses (about 500 poses); the better interaction what we get was for **7** and **8**, that have intermediate inhibition of 100 μM, better than **9** ligand. On the other hand docking against HDAC2; Vorinostat (VS or SAHA) has scored approximately 35 nM (Table.1) while other ligands have given less extent of affinity scores, **7** took the second place after **VS** by scoring 8 μM. Due to the limitation of access deep into HDAC2, **7** takes the lead among biguanides because of its size, however some poses were successful to be close enough from Zn atom making coordinate bond, although, biguanide based ligands have failed to be as potent as **VS**, but have showed excellent blockage of the binding pocket as well as a cross interaction with HDACs. Finally docking against HDAC3; VS has scored approximately 3.5 nM, while other ligands have given less extent of affinity scores, **9** took the second place after **VS** by scoring 169 μM better than others **7** or **8** which gave very weak interaction.

The identification of these compounds was carried out by ATR-IR through the disappearance of bands of the lost functional groups and the appearance of new bands of the newly formed functionalities. The resulted amide bond appeared obviously as band in the usual amide region around 1660 as shown below. The removal of boc moiety results in disappearance of carbamate carbonyl and tri-methyl bands and appearance of multiple bands of primary ammonium salts. The coupling with dicyandiamide resulting in multiple NH and NH_2 bands through region above 3000 and the appearance of C = N double bond bands (Table 2).

The most important procedure of identification is the HNMR study which showed structural conformity with the resulted chemical shifts, splitting pattern and integrations (Table 3).

3.2. Biological study

The study of cytotoxic effect of VS, MET and biguanide analogues against cancer cells was carried out MCF-7 as an in vitro cell line of HER2 + breast cancer. The activity of these analogues was tested by studying their ability to inhibit the proliferation of cancer cells. MTT assay method was the first widely accepted easy method used to measure cell proliferation and cytotoxic effect of the tested analogues. Even though it is widely used, the MTT stain was replaced by SRB (sulforhodamine B) stain for studying the cytotoxic effects which gives more consistent, less variant data and more accurate results but it was not available at study period. The overall results of the newly synthesized compounds showed highly significant cytotoxic activity against the human breast can-

Table 1
The results of interactions of the ligands with the three histone deacetylases.

Code	Targeted receptor	Estimated affinity	Hydrogen bonds	Best non- hydrogen bond interaction	ΔG of non-hydrogen bond interaction(kJ/mol)	Coordinating bond length (with Zinc) (Å)
VS	HDAC1	1.5 μM	His178 (1.93 Å) Leu271 (1.86 Å)	His178/Tyr303 Phe150	−9.2	2.23
7	HDAC1	104 μM	Asp99 (1.97 Å)	His178, Gly300, His140	−8.3	2.29
8	HDAC1	101 μM	Asp99 (1.93 Å)	His178, Tyr33	−7.6	2.33
9	HDAC1	1.0 M	Tyr303 (1.77 Å)	Nothing special	Non	non
VS	HDAC2	34 nM	Asp104 (1.88 Å) His145 (2.10 Å), His146 (1.92 Å), Tyr308 (2 Å)	His145, Gly306	−11.6	2.18
7	HDAC2	8.4 μM	2H-bond with Asp104 (1.87 Å and 2 Å), His183 (1.92 Å)	Phe210, Phe155	−4.4	No bond
8	HDAC2	23 μM	2H-bonds with Asp104 (2.02 Å and 1.90 Å), His183 (1.93 Å)	Leu 276	−3.9	No bond
9	HDAC2	28 μM	Asp104 (1.97 Å) Glu103 (1.92 Å)	Gly154, Phe210, Phe155	−4.9	No bond
VS	HDAC3	3.5 nM	Gly143 (1.75 Å), His172 (1.91 Å), Phe200 (1.82 Å)	His172, Tyr298	−5.5	1.98
7	HDAC3	1,000 M	Gly143 (2.2 Å), questionable bond!	His172	−6.7	1.98
8	HDAC3	1.3 mM	Asp93 (1.90 Å), His172 (1.94 Å)	Phe144, His172, Tyr298	−3.9	No bond
9	HDAC3	169 μM	Asp93 (2.08 Å), Gly143 (1.70 Å)	Leu133, Gly295	−7.2	2

Table 2
The characteristic IR data of the synthesized compounds.

No.	Characteristic IR data	The important bands
1	3329, 3267, 3202, 3140, 3082, 2987, 2866, 1686, 1659, 1600, 1492, 1531 and1165	Carbamate (1686) Amide I (1659)
2	3317, 3275, 3217, 3159, 3082, 2987, 2866, 1686, 1659, 1600, 1492, 1531 and 1165	Carbamate (1686) Amide I (1659)
3	3309, 3256, 3194, 3121, 3063, 2978, 2874, 1666, 1600, 1489, 1531 and 1169	Amide I (1666)
4	3236–3128, 3078, 3032–2812, 2812–2000, 2920, 2862, 1666, 1601, 1489, 1601 and 1543	3032–2812 band of NH3+ (broad) 2812–2000 Multiple bands of NH3 + group
5	3252, 3013, 3013–2812, 2812–2000, 2955, 2870, 1651, 1616,1508, 1562, 1470 and 1543	3013–2812 band of NH3 + group (broad) 2812–2000 Multiple bands of NH3 + group
6	3252–3182, 3001–2870, 3001, 2870–2000, 2947, 2870, 1659, 1609 and 1493, 1593, 1470 and 1539	3001–2870 band of NH3 + group (broad) 2870–2000 Multiple bands of NH3 + group
7	3341, 3263, 3194, 3140, 3024, 2978, 2874, 1651, 1635, 1597, 1501 and 1543	1635C = N str. and NH bending of NH2 & NH2 + overlapped bands
8	3348, 3256, 3152, 3086, 3020, 2978, 2874, 1632, 1562, 1508, 1543	1632Carbonyl str. of anilide carbonyl (amide I), C = N str. band, C = N str. and NH bending of NH2 & NH2 + overlapped bands
9	3348, 3267, 3182, 3124, 3001, 2970, 2874, 1647, 1612, 1593, 1493, 1539	1612C = N str. and NH bending of NH2 & NH2 + overlapped bands

Table 3
The characteristic HNMR data for the newly synthesized compounds.

No.	Chemical shift, No. of protons(Multiplicity)
1	1.37,9H(s), 1.66–1.72,2H(p), 2.28–2.31,2H(t), 2.95–2.99,2H(q), 6.81–6.84,1H(t), 7.00–7.03,1H(t), 7.26–7.29,2H(t), 7.58–7.59,2H(d), 9.86,1H (s)
2	1.37,9H(s), 1.65–1.71,2H(p), 2.26–2.29,2H(t), 2.94–2.98,2H(q), 6.81–6.83,1H(t), 7.09–7.14,2H(t), 7.58–7.61,2H(m), 9.92,1H(s)
3	1.37,9H(s), 1.65–1.71,2H(p), 2.28–2.31,2H(t), 2.94–2.98,2H(q), 6.81–6.83,1H(t), 7.31–7.34,2H(m), 7.60–7.62,2H(d), 10.00,1H(s)
4	1.85–1.91,2H(p), 2.43–2.46,2H(t), 2.82–2.86,2H(t), 7.02–7.05,1H(d), 7.27–7.31,2H(t), 7.60–7.62,2(d), 7.95,3H(s), 10.12,1H(s)
5	1.86–1.89,2H(p), 2.43–2.46,2H(t), 2.81–2.85,2H(t), 7.13–7.16,2H(m), 7.63–7.64,2H(m), 7.96,3H(s), 10.23,1H(s)
6	1.83–1.91,2H(p), 2.44–2.47,2H(t), 2.81–2.85,2H(t), 7.25–7.37,2H(d), 7.65–7.68,2H(d), 7.96,3H(s), 10.33,1H(s)
7	1.88–1.94,2H(m), 2.46–2.49,2H(t), 2.83–2.86,2H(t), 7.00–7.04,3H(m), 7.26–7.29,2H(t), 7.64, 7.65,2H(d), 7.69,1H(s), 8.46,4H(br s), 10.29,1H(s)
8	1.83–1.91,2H(p), 2.42–2.46,2H(t), 2.81–2.85,2H(t), 7.00,2H(s), 7.11–7.16,2H(t), 7.62–7.65, 2H(m), 7.97,4H(s), 10.23,1H(s)
9	1.87–1.93,2H(m), 2.47–2.50,2H(t), 2.82–2.85,2H(t), 7.00–7.04,2H(s), 7.32–7.34,2H(d), 7.68–7.71,3H(m), 8.43,4H(br s), 10.50,1H(s)

Table 4
The IC_{50} of the SAHA, MET, **7**, **8** and **9.**

No.	Compound Name	IC50(μM) ± SD
1	MET	4901.4 ± 256*
2	SAHA	97.5 ± 6.75
3	7	155.75 ± 12.82*
4	8	99.18 ± 11.11
5	9	145.55 ± 8.55*

* represent a statistically significant different value of IC_{50} for the tested compound as compared with SAHA ($P < 0.01$).

cer cells. These results suggest the significant ability of these compounds to suppress the growth of cells in concentration dependent manner. Metformin as it is showed very weak activity on breast cancer cells with concentration of 4.9 mM IC50 while **VS** and other analogues showing moderate activity of concentration range 97.5–155.75 μM. The response and growth inhibition for the 3 analogues was somewhat different, the best result among them was for compound **8** with lower IC50 of 99.18 μM which is comparable with VS IC50 (97.5 μM) while both compounds **7** and **9** are with moderate activity but weaker than **VS** (Table 4, Figs. 3–9).

4. Conclusion

The breast cancer treatment is an objective target for many researches to find safe effective treatment to decrease its mortality

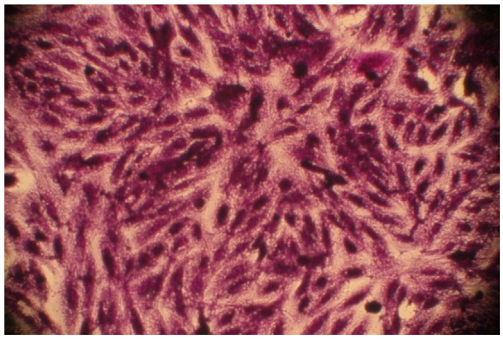

Fig. 2. Normal untreated MCF-7 Cells.

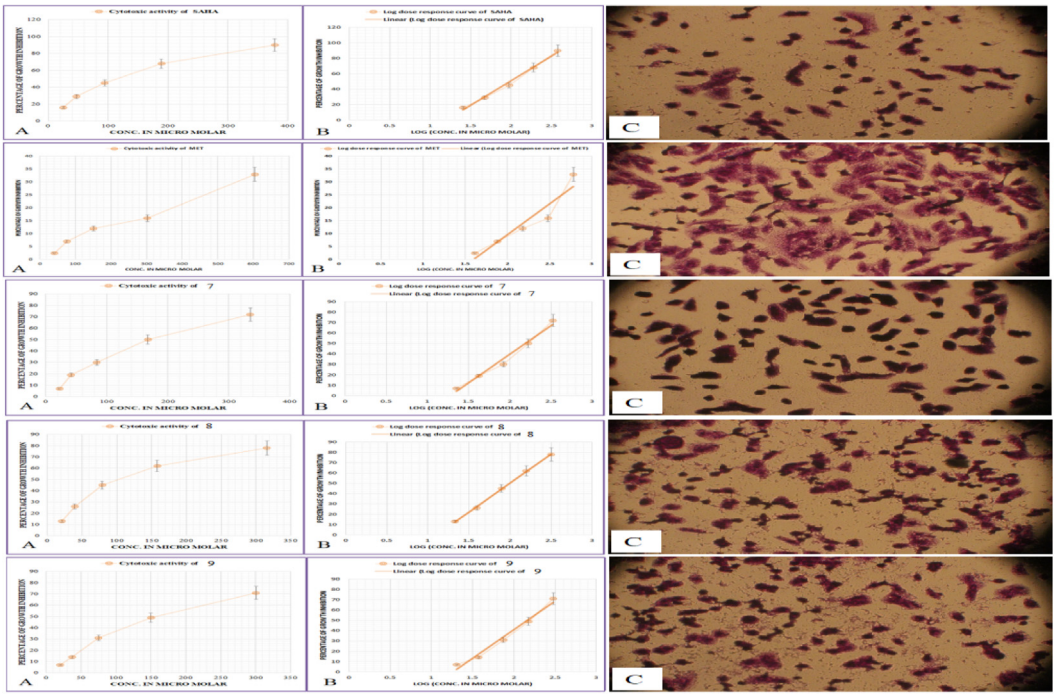

Fig. 3. Dose response (A) and log dose response (B) curves for the cytotoxic effect of SAHA, MET, **7**, **8** and **9** against MCF-7 cell line. The results were expressed as mean ± SD of the triplicate. The linear regression analysis of the log dose response curve showed a significant correlation between the log of the dose and the percentage of cell growth inhibition.

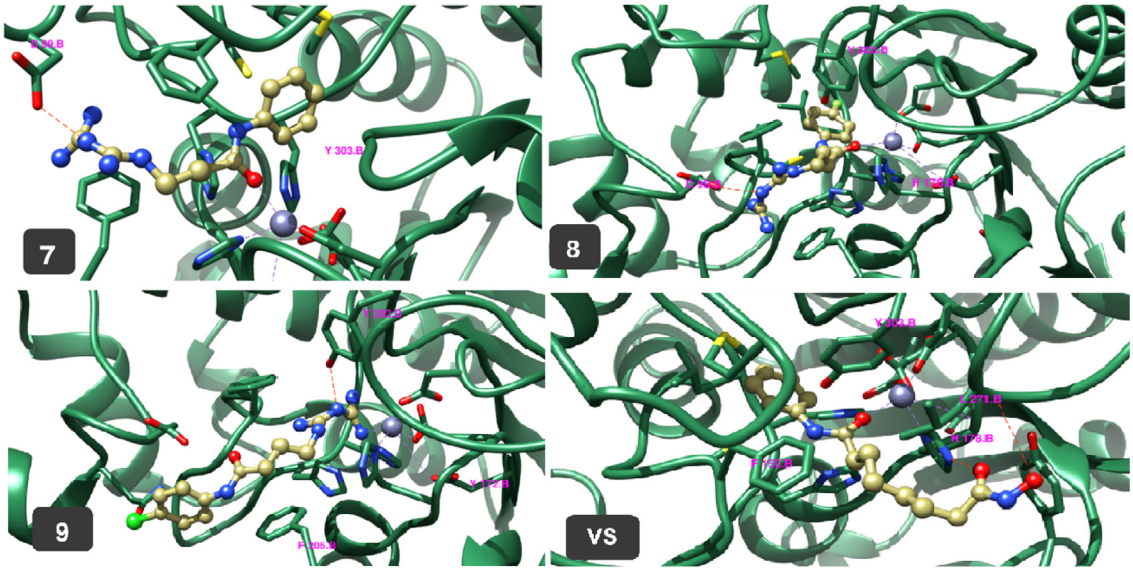

Fig. 4. The interaction of ligands with HDAC1 active site.

and morbidity through the discovery of novel classes of anticancer agents with distinct mechanism of action could be used individually or in combination. From the docking study it was concluded that biguanide moiety was very successful to bind tightly to HDACs by making numerous interaction modes. Through searching for allosteric binding site in case of HDAC2 may be could show better results with biguanides based ligands. Modification on amide moiety may lead to more likely better interaction with HDAC1. **8** seemed to have a prosperous future as an inhibitor for HDAC3, cell-based experiments are recommended for further investigation of its activity. Therefore these newly synthesized analogues may be represent an exploitable source of new anticancer agents fighting breast cancer. The therapeutic potential of these agents is fairly obvious suggesting a promising novel class of HADC inhibitors fighting breast cancer.

CRediT authorship contribution statement

Othman Makki Sagheer: Methodology, Investigation, Validation, Writing - review & editing. **Mohammed Hassan Mohammed:** Methodology, Investigation, Validation, Writing - review & editing.

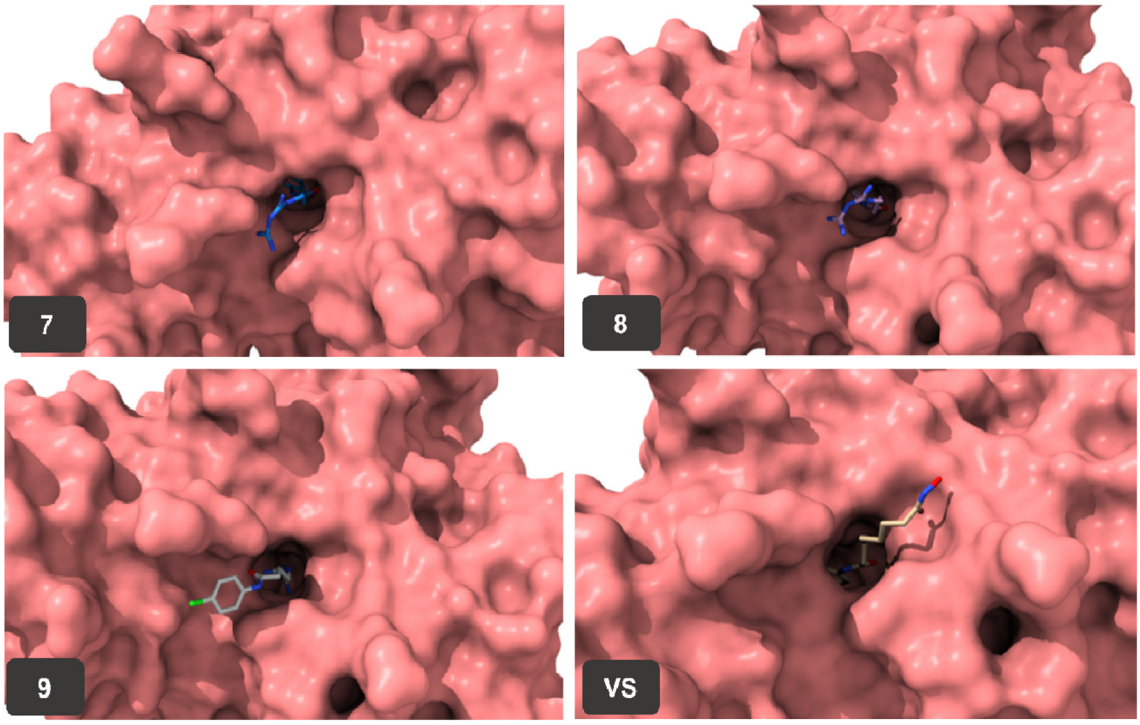

Fig. 5. The occupation of the binding pocket of HDAC1 by the ligands.

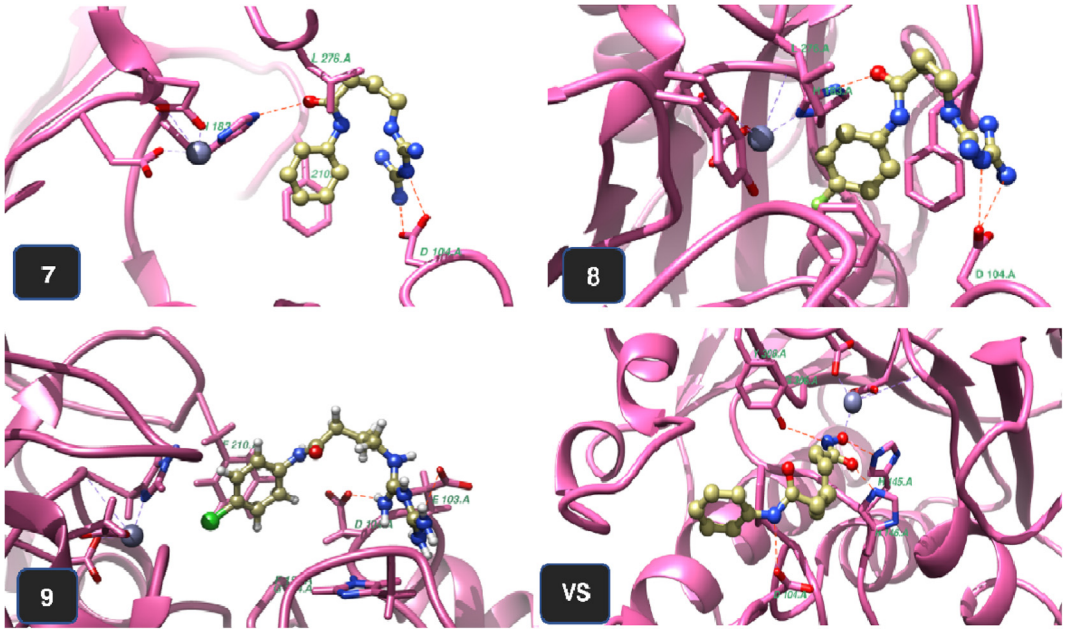

Fig. 6. The interaction of ligands with HDAC2 active site. In another hand, biguanide-ligands have competed **VS** in making fruitful interaction with HDAC1 and HDAC3.

Zaid O. Ibraheem: Visualization, Conceptualization, Investigation, Writing - review & editing, Formal analysis. **Jaafar S. Wadi:** Visualization, Conceptualization, Investigation, Writing - review & editing, Formal analysis. **Mustafa F. Tawfeeq:** Visualization, Conceptualization, Investigation, Writing - review & editing, Formal analysis.

Declaration of Competing Interest

The authors declare that they have no known competing financial interests or personal relationships that could have appeared to influence the work reported in this paper.

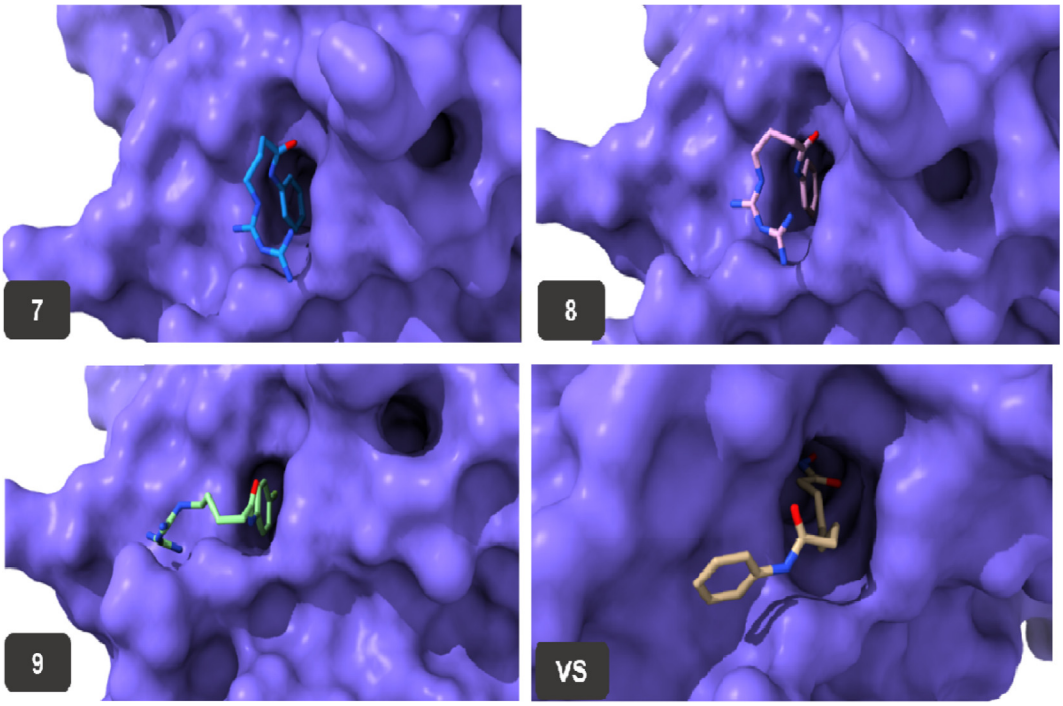

Fig. 7. The occupation of the binding pocket of HDAC2.

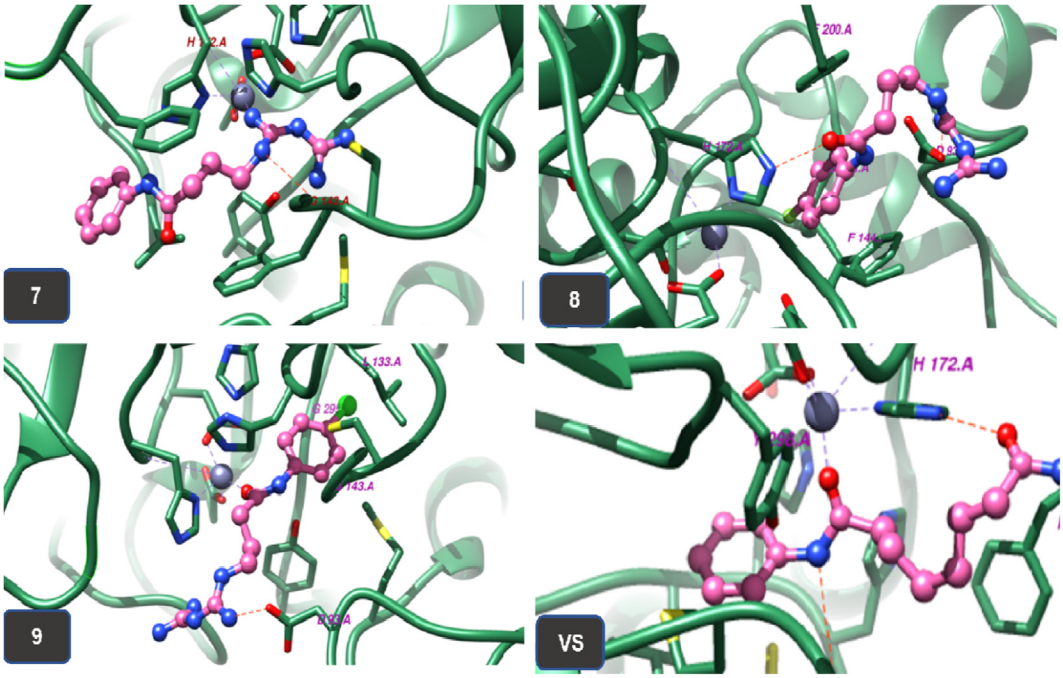

Fig. 8. The binding site of HDAC3 that has contained ligands **7–9** and VS.

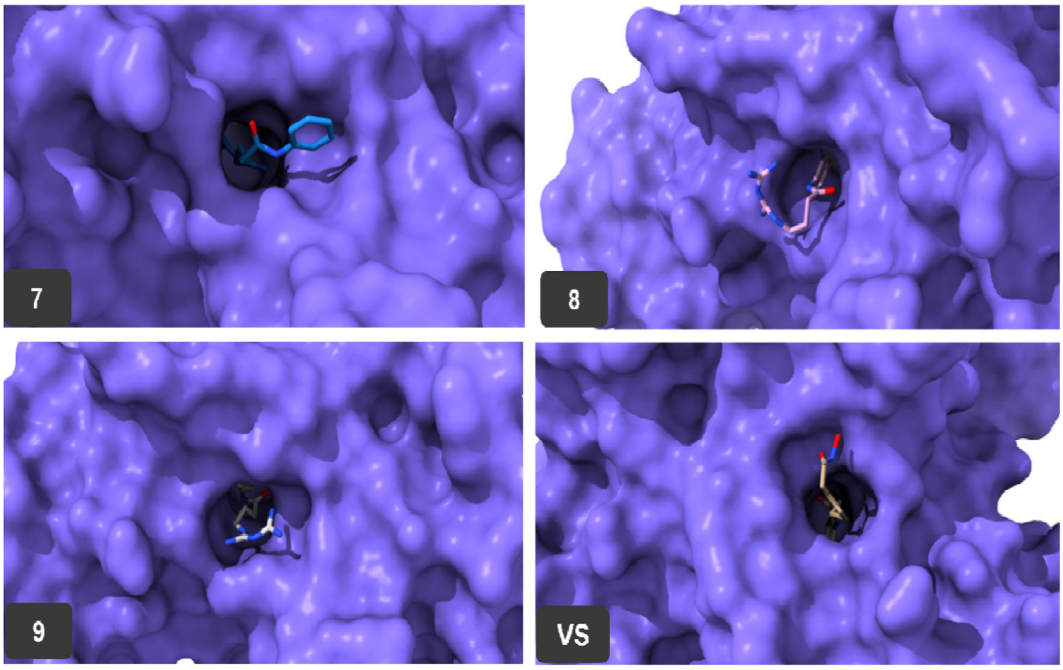

Fig. 9. Occupying the binding pocket of HDAC3 by ligands **7**–**9** as well as **Vs**.

References

[1] J. Ferlay et al., Cancer incidence and mortality worldwide: sources, methods and major patterns in GLOBOCAN 2012, Int. J. Cancer 136 (5) (2015) E359–E386.
[2] F. Bray et al., Global cancer statistics 2018: GLOBOCAN estimates of incidence and mortality worldwide for 36 cancers in 185 countries, CA Cancer J. Clin. 68 (6) (2018) 394–424.
[3] S.A. Armstrong, S. Henikoff, C.R. Vakoc, Chromatin Deregulation in Cancer, Cold Spring Harbor Laboratory Press, Cold Spring Harbor, New York, 2017, vii, 382 pages.
[4] E. Verdin, Histone Deacetylases: Transcriptional Regulation and Other Cellular Functions. Cancer Drug Discovery and Development, Humana Press, Totowa, 2006, xi N.J. 340.
[5] B. Biersack, S. Polat, M. Höpfner, Anticancer properties of chimeric HDAC and kinase inhibitors, Semin. Cancer Biol. (2020), https://doi.org/10.1016/j.semcancer.2020.11.005.
[6] X. Peng et al., Recent progress on HDAC inhibitors with dual targeting capabilities for cancer treatment, Eur. J. Med. Chem. 208 (2020) 112831.
[7] C. Cao et al., HDAC5-LSD1 axis regulates antineoplastic effect of natural HDAC inhibitor sulforaphane in human breast cancer cells, Int. J. Cancer 143 (6) (2018) 1388–1401.
[8] G. Borbely et al., Induction of USP17 by combining BET and HDAC inhibitors in breast cancer cells, Oncotarget 6 (32) (2015) 33623–33635.
[9] A.J.d. Ruijter et al., Histone deacetylases (HDACs): characterization of the classical HDAC family, Biochem. J. 370 (3) (2003) 737–749.
[10] H. Zhou et al., Design, virtual screening, molecular docking and molecular dynamics studies of novel urushiol derivatives as potential HDAC2 selective inhibitors, Gene 637 (2017) 63–71.
[11] M. Stahl et al., Epigenetics in cancer: a hematological perspective, PLoS Genet. 12 (10) (2016) e1006193.
[12] X. Bian et al., HDAC inhibitor suppresses proliferation and invasion of breast cancer cells through regulation of miR-200c targeting CRKL, Biochem. Pharmacol. 147 (2018) 30–37.
[13] H. Hess-Stumpp, Histone deacetylase inhibitors and cancer: from cell biology to the clinic, Eur. J. Cell Biol. 84 (2-3) (2005) 109–121.
[14] H. Fang et al., HDAC inhibitors induce proline dehydrogenase (POX) transcription and anti-apoptotic autophagy in triple negative breast cancer, Acta Biochim. Biophys. Sin (Shanghai) 51 (10) (2019) 1064–1070.
[15] P. Cheung, C.D. Allis, P. Sassone-Corsi, Signaling to chromatin through histone modifications, Cell 103 (2) (2000) 263–271.
[16] T.A. Miller, D.J. Witter, S. Belvedere, Histone deacetylase inhibitors, J. Med. Chem. 46 (24) (2003) 5097–5116.
[17] M. Choi et al., Association of insulin, metformin, and statin with mortality in breast cancer patients, Cancer Res. Treat. 53 (1) (2021) 65–76.
[18] M. Aljofan, D. Riethmacher, Anticancer activity of metformin: a systematic review of the literature, Future Sci. OA 5 (8) (2019) FSO410.
[19] J.C. Brown et al., Effect of exercise or metformin on biomarkers of inflammation in breast and colorectal cancer: a randomized trial, Cancer Prev. Res. (Phila) 13 (12) (2020) 1055–1062.
[20] L. Cheng et al., Metformin exhibits antiproliferation activity in breast cancer via miR-483-3p/METTL3/m(6)A/p21 pathway, Oncogenesis 10 (1) (2021) 7.
[21] G.N. Vaidya et al., Paradigm shift of "classical" HDAC inhibitors to "hybrid" HDAC inhibitors in therapeutic interventions, Eur. J. Med. Chem. 209 (2021) 112844.
[22] B. Elpern, Chemistry of the biguanides, Ann. N. Y. Acad. Sci. 148 (3) (1968) 577–586.
[23] P. Ray, Complex compounds of biguanides and guanylureas with metallic elements, Chem. Rev. 61 (4) (1961) 313–359.
[24] T. Noguchi et al., Convenient preparation of primary amides via activation of carboxylic acids with ethyl chloroformate and triethylamine under mild conditions, Chem. Lett. 42 (6) (2013) 580–582.
[25] D.M. Shendage, R. Fröhlich, G. Haufe, Highly efficient stereoconservative amidation and deamidation of α-amino acids, Org. Lett. 6 (21) (2004) 3675–3678.
[26] K. Narise et al., Optimization of biguanide derivatives as selective antitumor agents blocking adaptive stress responses in the tumor microenvironment, Drug Des. Develop. Ther. 8 (2014) 701.
[27] S. Mayer et al., An expedient and facile one-step synthesis of a biguanide library by microwave irradiation coupled with simple product filtration. Inhibitors of dihydrofolate reductase, J. Comb. Chem. 6 (5) (2004) 776–782.
[28] S. Fortun, A.R. Schmitzer, The chemistry of biguanides: from synthetic routes to applications in organic chemistry, Can. J. Chem. 98 (6) (2020) 251–260.
[29] J. Kirkland, Development of some stationary phases for reversed-phase HPLC, J. Chromatogr. A 1060 (1-2) (2004) 9–21.
[30] M. Koshioka et al., Reversed-phase C18 high-performance liquid chromatography of acidic and conjugated gibberellins, J. Chromatogr. A 256 (1983) 101–115.
[31] K.S. Khashan et al., Synthesis, characterization and evaluation of anti-bacterial, anti-parasitic and anti-cancer activities of aluminum-doped zinc oxide nanoparticles, J. Inorg. Organomet. Polym Mater. 30 (9) (2020) 3677–3693.
[32] M. Jabir et al., Linalool-loaded glutathione-modified gold nanoparticles conjugated with CALNN peptide as apoptosis inducer and NF-κB translocation inhibitor in SKOV-3 Cell Line, Int. J. Nanomed. 15 (2020) 9025.
[33] M.S. Jabir et al., Supermagnetic Fe3O4-PEG nanoparticles combined with NIR laser and alternating magnetic field as potent anti-cancer agent against human ovarian cancer cells, Mater. Res. Express 6 (11) (2019) 115412.
[34] H.N.K. Al-Salman et al., 2-Benzhydrylsulfinyl-N-hydroxyacetamide-Na extracted from fig as a novel cytotoxic and apoptosis inducer in SKOV-3 and AMJ-13 cell lines via P53 and caspase-8 pathway, Eur. Food Res. Technol. 246 (8) (2020) 1591–1608.
[35] A.G. Al-Ziaydi et al., Newcastle disease virus suppress glycolysis pathway and induce breast cancer cells death, VirusDisease 31 (3) (2020) 341–348.
[36] K.S. Khashan, M.S. Jabir, F.A. Abdulameer, Carbon nanoparticles prepared by laser ablation in liquid environment, Surf. Rev. Lett. 26 (10) (2019) 1950078.
[37] S.H. Kareem, A.M. Naji, Z.J. Taqi, M.S. Jabir, Polyvinylpyrrolidone loaded-MnZnFe 2 O 4 magnetic nanocomposites induce apoptosis in cancer cells through mitochondrial damage and P 53 pathway, J. Inorg. Organomet. Polym Mater. 30 (12) (2020) 5009–5023.

[38] M.S. Jabir et al., Green synthesis of silver nanoparticles using Annona muricata extract as an inducer of apoptosis in cancer cells and inhibitor for NLRP3 inflammasome via enhanced autophagy, Nanomaterials 11 (2) (2021) 384.
[39] H.M. Waheeb, G.M. Sulaiman, M.S. Jabir, Effect of hesperidin conjugated with golden nanoparticles on phagocytic activity: in vitro study, in: AIP Conference Proceedings. AIP Publishing LLC, 2020.
[40] A.M. Al-Shammari et al., Galangin enhances gold nanoparticles as anti-tumor agents against ovarian cancer cells, in: AIP Conference Proceedings, AIP Publishing LLC, 2020.
[41] I. Reulecke et al., Towards an integrated description of hydrogen bonding and dehydration: decreasing false positives in virtual screening with the HYDE scoring function, ChemMedChem: Chemistry EnablingDrug Discovery 3 (6) (2008) 885–897.